Lawrence Berkeley National Laboratory

Lawrence Berkeley National Laboratory

Title

Metastable Solid Solution Phases in the LiFePO4/FePO4 System

Permalink

https://escholarship.org/uc/item/5q21h65j

Authors

Chen, Guoying Chen
Song, Xiangyun
Richardson, Thomas J.

Publication Date

2006-01-02

Peer reviewed

eScholarship.org Powered by the California Digital Library
University of California

Metastable Solid Solution Phases in the $LiFePO_4/FePO_4$ System

Guoying Chen[*], Xiangyun Song and Thomas J. Richardson[*, z]

Environmental Energy Technologies Division

Lawrence Berkeley National Laboratory

Berkeley, California 94720 USA

Abstract

Solid solution behavior in the $LiFePO_4$-$FePO_4$ system was investigated using x-ray powder diffraction. A substantial dependence upon crystal size and morphology was observed. Partially delithiated samples of 4 x 2 x 0.2 μm^3 hydrothermally synthesized olivine-type Li_xFePO_4 crystals containing only the two end-member phases were heated to form single-phase solid solutions. In samples with $x > 0.6$, a line phase with composition Li_yFePO_4 ($y = 0.60 \pm 0.04$) appeared as an intermediate during the transformation of the two-phase mixtures to single-phase Li_xFePO_4. This phase then precipitated during cooling along with $LiFePO_4$ and persisted at ambient temperature. Transmission electron microscopy indicated that upon cooling, phase separation occurred within the crystals along the *b* direction (space group P*nma*), with $LiFePO_4$ forming at the (010) surfaces. More complex behavior was found for samples with $x < 0.6$ and for crystals of smaller dimensions.

---

[*] Electrochemical Society Active Member

[z] E-mail: tjrichardson@lbl.gov

Introduction

Lithium iron phosphate, $LiFePO_4$, with a phospho-olivine structure has become an important cathode material for rechargeable lithium batteries. Because it is made from abundant and inexpensive elements, is environmentally friendly, and has excellent thermal stability, it is expected that it will be used in large-scale battery applications. The theoretical capacity of 170 mAh/g can be utilized with a nearly flat cell voltage of about 3.4 V vs. Li^+/Li. The reaction proceeds *via* a first order phase transition in which $LiFePO_4$ is converted to $FePO_4$.[1] As both $LiFePO_4$ and $FePO_4$ have poor electronic and ionic conductivities,[2-3] the existence of room temperature solid solution phases with small Li nonstoichiometry during the phase transition has been proposed to explain the surprisingly facile reaction.[4-5] Yamada et al.[6] recently reported the detection of mixed-valent intermediate phases, $Li_\alpha FePO_4$ ($0 < \alpha < 0.05$) and $Li_{1-\beta}FePO_4$ ($0.89 < 1 - \beta < 1$), outside the room temperature miscibility gap, and proposed that improvements in rate capability could be achieved by increasing α and/or $1 - \beta$. Isolation and characterization of the pure ambient temperature solid solutions has not yet been achieved.

The transformation of two-phase mixtures of $LiFePO_4$ and $FePO_4$ to single-phase Li_xFePO_4 solid solutions at elevated temperatures was recently reported by Delacourt et al.[7-8] and by Dodd et al.[9-10] Although the phase diagrams from these two studies differ in some details, they establish the existence of solid solution phases at all values of x, that with $x \approx 0.6$ being stable at the lowest temperature (150-200° C) and appearing as an intermediate during cooling. Refinement of room temperature diffraction patterns of quenched samples containing this phase shows that it is disordered, with shorter average

Fe-O bonds and longer average M1-O lengths (M1 refers to Li when present and to the center of the Li site when it is vacant).[8]

We recently studied the $LiFePO_4/FePO_4$ phase transition mechanism in hydrothermally synthesized crystals with a characteristic shape and uniform size distribution.[11] The use of such high quality crystals allows us to study the behavior of the material at the crystallite level. When chemical agents are used to extract or insert lithium, the composition is relatively uniform among particles as compared to that of agglomerated materials with a wide crystallite size distribution. We report here an investigation of solid solution formation upon heating and phase separation upon cooling of partially delithiated crystals.

Experimental

Hydrothermal Synthesis

Discrete $LiFePO_4$ crystals with a uniform size distribution were synthesized by using the hydrothermal method described by Yang et al.[12] $FeSO_4$ (99%, Aldrich) and H_3PO_4 (85%, J. T. Baker) were mixed in deoxygenated and deionized water, and LiOH (Spectrum) solution was added slowly to the mixture to give an overall Fe: P: Li ratio of 1: 1: 3. After stirring under nitrogen for about 5 min, the reaction mixture was transferred to a Parr reactor, which was purged by nitrogen and heated at 220 ^oC for 3 h. On cooling to room temperature, the off-white precipitate was filtered, thoroughly washed with deionized water, and dried at 60 ^oC under vacuum for 24 h. Delithiated crystals were obtained by stirring the $LiFePO_4$ in a solution of bromine in acetonitrile for 1 h, with the molar ratio adjusted to achieve the desired stoichiometry.

X-ray Diffraction

X-ray diffraction (XRD) patterns were acquired in reflection mode using a Panalytical Xpert Pro diffractometer equipped with monochromatized Cu Kα radiation. The scan rate was 0.0025°/s from 10° to 70° 2θ in 0.01° steps. The phase ratio in *x* $LiFePO_4$/(1-*x*) $FePO_4$ two-phase mixtures was determined from XRD data using Riqas Rietveld refinement software (MDI). Temperature-controlled XRD studies were performed under Argon on the same diffractometer equipped with an Anton Parr HTK 1200 hot stage. The samples were heated at a rate of 5 ^oC/min, and XRD patterns were recorded after holding at each temperature for 1h, using a scan rate of 0.006°/s and a step size of 0.05°. The same procedure was used during the cooling process. Two-phase *x*$LiFePO_4$/(1-*x*)$FePO_4$ samples were also subjected to the same heating and cooling steps in a tube furnace under flowing argon, then studied at room temperature. Rietveld refinement of the XRD data was used to determine the phase-composition of the samples, as well as the crystallographic parameters of the obtained phases.

Transmission electron microscopy

Transmission electron microscopy (TEM) and high-resolution transmission electron microscopy (HRTEM) experiments were carried out at the National Center for Electron Microscopy (NCEM) at LBNL, using a Philips CM200 field emission microscope operating at 200 kV. Samples for TEM were gently ground to decrease the size of the crystals, and then dispersed in ethanol. The resulting dispersion was transferred to a holey carbon film fixed on a 3 mm copper grid. Electron diffraction patterns were collected using the selected area electron diffraction (SAED) technique.

Fourier transforms of the HRTEM images were carried out by using DigitalMicrography^{TM} software (Gatan Inc., v 3.3.1).

Results and Discussion

XRD phase analysis

Rietveld refinement of the XRD pattern obtained from hexagonal $LiFePO_4$ crystals measuring 2 μm x 0.2 μm x 4 μm along the *a*, *b*, and *c*-axes, respectively, gave unit cell parameters a = 10.3342(3) Å, b = 6.0017(2) Å, c = 4.6951(1) Å, and V = 290.2 Å^3, in good agreement with the literature values.[13] A series of crystal samples with lithium content x of 0.14, 0.38, 0.50, 0.60, 0.65, 0.73, 0.77 and 0.85 were prepared by oxidation with stoichiometric amounts of bromine in acetonitrile. XRD patterns of these samples showed that the partially oxidized samples consisted of two-phase mixtures of the end members in the ratio xLiFePO$_4$/(1-x)FePO$_4$. Selected area electron diffraction (SAED) studies showed that among crystals in a given sample, there was little variation in the phase ratio. The thermal behavior of these samples was studied either by *in-situ* temperature-controlled XRD, or by *ex-situ* XRD after heating the samples to form solid solution phases in a tube furnace, and then cooling them to room temperature under argon. The XRD patterns for x = 0.50, 0.65, 0.77 during heating and cooling are shown in Fig. 1. The peaks marked with an asterisk correspond to an unidentified impurity phase that does not participate in the formation or decomposition of solid solution phases. In each case, significant structural changes occurred on heating to about 200 ^oC, in accord with the reports of Delacourt et al., Dodd et al., and Ellis et al.[14] As the peak intensities from $LiFePO_4$ and $FePO_4$ decreased, a new set of peaks from a line phase, Li_yFePO_4,

emerged. Comparison of the XRD patterns at 200 ^{o}C (Fig. 1d) indicated that this line phase was a common intermediate that appeared during heating with a constant composition but in increasing amount until the initial quantity of $FePO_4$ was consumed. Thereafter, the solid solution phase became more Li-rich as the remaining $LiFePO_4$ was absorbed. Based on the phase ratios obtained from XRD refinements and the known global Li content in the samples, y was determined to be 0.60 ±0.04.

In contrast to the earlier reports, we did not observe significant peak broadening during the transition. Delacourt et al. attributed the phenomenon to the presence of Li gradients within the crystal structure during the transformation of the two-phase mixture to the single-phase solid solution. In fact, this could result from non-uniform distribution of Li within the sample. For samples composed of aggregated particles with a wide primary size distribution, it is likely that some crystallites contain less lithium than others. This could result in local lithium contents below x = 0.5, a regime in which we observed behavior different from that described here. Our use of uniform, discrete particles avoided wide variations in Li content and allowed us to detect the intermediate line phase during the transformation process.

The formation temperature of phase pure solid solution was typically around 300 ^{o}C, with a slight variation among the samples with different Li content. Upon cooling, phase separation was typically observed at around 150 ^{o}C. For samples with $x > 0.6$, the solid solution phase disproportionated into a two-phase mixture of $LiFePO_4$ and the same intermediate phase, $Li_{0.60}FePO_4$, that was observed during the heating process. The XRD patterns of the Li_xFePO_4 samples with x = 0.65, 0.73, 0.77, and 0.85 after cooling to room temperature are compared in Fig. 2a. The 211/020 peak intensities (which are nearly

coincident for all phases) show the relative amounts of the two phases, which depend only on the global Li content. Refinement of the entire patterns gave 85 % of the intermediate phase in the sample with $x = 0.65$, 67 % for $x = 0.73$, 57 % for $x = 0.77$, and 38 % for $x = 0.85$. For samples with lithium content below 0.6 (Fig. 2b), cooling of the Li_xFePO_4 solid solutions produced more complicated mixtures. 83 % $Li_{0.60}FePO_4$ and 17 % $FePO_4$ were formed when $x = 0.50$. For $x = 0.38$, the product was 2 % $LiFePO_4$, 25 % $Li_{0.60}FePO_4$, 43 % $FePO_4$, and 30 % a new intermediate phase, Li_zFePO_4. For $x = 0.14$, only two phases were present: 59 % $FePO_4$ and 41% Li_zFePO_4. Refinement of the XRD patterns gave $z = 0.34 \pm 0.04$. This phase also exhibited room temperature stability.

Fig. 3 summarizes the lattice parameters and unit cell volumes of the four phases after cooling to room temperature, derived from XRD refinement of the samples with $x =$ 0, 0.14, 0.38, 0.50, 0.65, 0.73, 0.77, 0.85, and 1. Although the values of *b* for $Li_{0.60}FePO_4$ and $Li_{0.34}FePO_4$ are approximately those expected for a linear variation with Li content, *a* and *c* and the unit cell volumes of the solid solution phases are substantially closer to those of $LiFePO_4$, possibly due to the strong interaction between electrons and atoms in the system and the difficulty of accommodating both Fe^{2+} and Fe^{3+} ions in close proximity.[4,7] There is some variation in the *a* and *c* values for $Li_{0.60}FePO_4$ in the two-phase samples containing both this phase and $LiFePO_4$. As the amount of $LiFePO_4$ increases, the *a* and *c* parameters shift toward those of the fully lithiated phase, while *b* is unaffected. The *b* parameter is highly sensitive to variation in Li content,[7] so that if this shift were due to a change in stoichiometry, it would be reflected by a similar shift in the value of *b*. A more plausible explanation is the presence of residual stress between the two phases in the *ac* plane. This is further supported by the small shifts in the $LiFePO_4$

parameters toward those of the solid solution when only a small amount of $LiFePO_4$ is present ($x = 0.65$).

As we observed the presence of $Li_{0.60}FePO_4$ in samples with varying Li content during heating and cooling and even at room temperature, it seems that this particular intermediate phase possesses unusual thermodynamic and kinetic stability. The phase diagram of Li_xFePO_4 reported by Dodd et al. showed $x = 0.6$ as the eutectoid point, and Delacourt et al. reported $Li_{0.64}FePO_4$ as an important intermediate phase during the cooling process. In both of those reports, however, the intermediate phases quickly disproportionated to the end members when the sample was aged at room temperature. In contrast, $Li_{0.60}FePO_4$ is quite stable in our cooled crystals, even after 5 months (Fig. 4). Neither very slow cooling nor long-term annealing at 150 °C were found to stimulate further phase separation.

We attempted to obtain a phase pure room temperature $Li_{0.60}FePO_4$ solid solution sample by heating delithiated crystals with $x = 0.60$. The patterns from the temperature-controlled XRD data experiment are shown in Fig. 5. As before, $Li_{0.60}FePO_4$ appeared at about 200 ^oC, and was the only phase present at 325^oC. The solid solution maintained its phase purity until the sample had cooled to 100 °C, but then slowly began to disproportionate into a three-phase mixture containing $Li_{0.60}FePO_4$, $LiFePO_4$ and $FePO_4$. After aging at room temperature for two weeks, about 20 % of the $Li_{0.60}FePO_4$ had decomposed to $LiFePO_4$ and $FePO_4$. Apparently, the presence of some $LiFePO_4$ stabilizes $Li_{0.60}FePO_4$ during the cooling process.

Domain structure from TEM

In order to understand the metastability of the room-temperature solid solution in our crystal samples, we carried out detailed transmission electron microscopy (TEM) studies on cooled Li_xFePO_4 samples with $x = 0.65$ and 0.77. In both cases, SAED showed the presence of both $LiFePO_4$ and $Li_{0.60}FePO_4$ in individual crystals, with uniform phase ratios when sampled at different locations on the large (*ac*) faces. High-resolution (HRTEM) images were obtained on a small, thin $Li_{0.77}FePO_4$ crystal, in which inner layers of the crystal were exposed due to breakage (Fig. 6a). The HRTEM image and the reciprocal lattice derived by Fourier transformation (inset) of region A are shown in Fig. 6b. The darker and lighter areas correspond to thicker and thinner portions of the crystal, respectively. The lattice spacings of the darker portion of region A correspond to $LiFePO_4$ and $Li_{0.60}FePO_4$, with two sets of spots relating to $LiFePO_4$ domains, each rotated by an equal amount but in opposite directionsrelative to those for $Li_{0.60}FePO_4$. The lighter part of region A contains $Li_{0.60}FePO_4$ and only one set of spots due to $LiFePO_4$. Fig. 6c shows the HRTEM and the reciprocal lattice images derived from Fourier transforms of area B. In this case, the darker region consists of $LiFePO_4$ and $Li_{0.60}FePO_4$, while the lighter area is $LiFePO_4$ alone.

Before heating, the partially delithiated crystals consist of alternating domains of $LiFePO_4$ and $FePO_4$ with phase boundaries lying in the *bc* plane.[11] A solid solution can be formed either by internal diffusion of Li ions that includes some component in the *a* direction, or by external exchange of Li between particles and between domains within particles. Our results indicate that upon cooling, the solid solution disproportionates into the fully lithiated phase and a partially lithiated intermediate phase *via* lithium ion movement along the *b* direction, with phase boundaries lying in the *ac* plane. Further,

$LiFePO_4$ appears to form at the outer surface of the crystal, while the inner part of the crystal loses Li until the stoichiometry $Li_{0.60}FePO_4$ is reached. The crystals studied here have large *ac* faces which represent ca. 85 % of the crystal surface. Since the lattice mismatch in the *ac* plane between $Li_{0.60}FePO_4$ and $FePO_4$ is much larger than that for $Li_{0.60}FePO_4$ and $LiFePO_4$, one would expect a higher energy barrier to formation of $FePO_4$. The solid solution behavior of somewhat smaller crystals (1 μm x 0.2 μm x 1.5 μm) with the same morphology was identical. Separation into a larger number of phases, however, including other intermediate phases and $FePO_4$, was observed at room temperature in crystals with still smaller *ac* dimensions (0.3 μm x 0.2 μm x 0.5 μm). Such multiphase separation also occurred when the larger crystals were ground prior to delithiation and heating, whereas it did not take place in a sample ground after delithiation, heating and cooling. Thus, the cumulative strain energy at the $Li_{0.60}FePO_4/LiFePO_4$ phase boundary may contribute to the stabilization of the metastable solid solution phase during cooling. Yamada et al.[6] reported that formation of room temperature solid solution phases was somewhat suppressed in larger particles.

The linewidths of the XRD peaks attributed to $Li_{0.60}FePO_4$ at both high and low temperatures are similar to those of the end members in the starting materials. Aside from shifts due to thermal expansion, no significant differences were found between the high and low temperature XRD patterns of $Li_{0.60}FePO_4$. Attempts refine atom positions using the space group P*nma*, however, led to some unreasonable bond distances due to the presence of a two very different Fe ions. Although no superlattice reflections were detected by powder XRD, some additional spots were observed in SAED patterns.

Conclusions

Two metastable solid solution phases were shown to persist in highly crystalline Li_xFePO_4. $Li_{0.60}FePO_4$ was formed during both heating and cooling of samples with $x \approx 0.6$ or greater. During cooling of single-phase samples consisting of crystals with large *ac* faces, $Li_{0.60}FePO_4$ and $LiFePO_4$ formed by migration of Li in the *b* direction within the crystals. The latter phase was formed at the *ac* surface, while $Li_{0.60}FePO_4$ was stabilized in the interior of the crystals and may persist indefinitely at room temperature. The basis of the inherent stability of $Li_{0.60}FePO_4$ and $Li_{0.34}FePO_4$ and the significance of their stoichiometries remain unclear. A paper detailing spectroscopic characterizations of solid solution samples is in preparation.

Acknowledgements

We thank the National Center for Electron Microscopy at LBNL for the use of TEM facilities, and Dr. Charles Delacourt for valuable discussions. This work was supported by the Assistant Secretary for Energy Efficiency and Renewable Energy, Office of FreedomCAR and Vehicle Technologies of the U. S. Department of Energy under Contract No. DE-AC02-05CH11231.

References

[1] A. K. Padhi, K.S. Nanjundaswamy, and J.B. Goodenough, *J. Electrochem. Soc.*, **144**, 1188 (1997).

[2] P. S. Herle, B. Ellis, N. Coombs, and L. F. Nazar, *Nat. Mater.*, **3**, 147 (2004).

[3] P.P. Prosini, M. Lisi, D. Zane, and M. Pasquali, *Solid State Ionics*, **148**, 45 (2002).

[4] A. Yamada, H. Koizumi, N. Sonoyama, and R. Kanno, *Electrochem. Solid-State Lett.*, **8**, A409 (2005).

[5] V. Srinivasan and J. Newman, *Electrochem. Solid-State Lett.*, **9**, A110 (2006).

[6] A. Yamada, H. Koizumi, S.-I. Nishimura, N. Sonoyama, R. Kanno, M. Yonemura, T. Nakamura, and Y. Kobayashi, *Nat. Mater.*, **5**, 357 (2006).

[7] C. Delacourt, P. Poizot, J.-M. Tarascon, and C. Masquelier, *Nat. Mater.*, **4**, 254 (2005).

[8] C. Delacourt, J. Rodrígues-Carvajal, B. Schmitt, J.-M. Tarascon, and C. Masquelier, *Solid State Sci.*, **7**, 1506 (2005).

[9] J. L. Dodd, R. Yazami, and B. Fultz, *Electrochem. Solid-State Lett.*, **9**, A151 (2006).

[10] R. Stevens, J. L. Dodd, M. G. Kresch, R. Yazami, B. Fultz, B. Ellis, and L. F. Nazar, *J. Phys. Chem. B*, **110**, 22732 (2006).

[11] G. Chen, X. Song, and T. J. Richardson, *Electrochem. Solid-State Lett.*, **9**, A295 (2006).

[12] S. Yang, P. Y. Zavalij and M. S. Whittingham, *Electrochem. Commun.*, **3**, 505 (2001).

[13] A. S. Andersson, B. Kalska, L. Haggstrom, and J. O. Thomas, *Solid State Ionics*, **130**, 41 (2000).

[14] B. Ellis, L. K. Perry, D. H. Ryan, and L. F. Nazar, *J. Am. Chem. Soc.*, **128**, 11416 (2006).

Figure captions

1. X-ray diffraction patterns of Li_xFePO_4 samples during heating and cooling. a) x = 0.50, b) x = 0.65, and c) x = 0.77. Initial patterns are at the bottom. d) comparison of the three samples at 200 ^oC during heating. Vertical lines indicate the positions of solid solution 211/020 reflections.
2. X-ray diffraction patterns of Li_xFePO_4 samples after cooling to 25 ^oC. a) $0.65 < x < 0.85$, b) $0.14 < x < 0.65$. Insets: variation in 211/020 peak intensities of $LiFePO_4$ and $Li_{0.60}FePO_4$ with x.
3. Lattice parameters and cell volumes of the phases present in cooled Li_xFePO_4 samples. ▲ $LiFePO_4$, ♦ $Li_{0.60}FePO_4$, ■ $Li_{0.34}FePO_4$, ● $FePO_4$. Standard deviations of the refined lattice parameters were generally less than 0.001 Å, and all were less than 0.0015 Å.
4. X-ray diffraction patterns of cooled $Li_{0.65}FePO_4$ sample during aging at ambient temperature.
5. X-ray diffraction patterns of $Li_{0.60}FePO_4$ sample during heating and cooling.
6. Transmission electron microscopy. a) TEM image of cooled $Li_{0.77}FePO_4$ crystal, b) HRTEM and reciprocal lattice images of area **A**, c) HRTEM and reciprocal lattice images of area **B**. An a/c ratio of 2.15 corresponds to $Li_{0.60}FePO_4$, 2.19 to $LiFePO_4$.

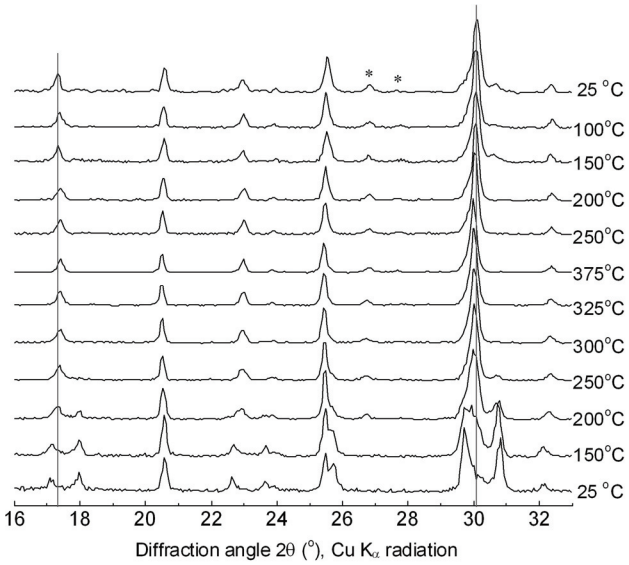
*
*
25 °C
100°C
150°C
200°C
250°C
375°C
325°C
300°C
250°C
200°C
150°C
25 °C
16
18
20
22
24
26
28
30
32
Diffraction angle 2θ (°), Cu Kα radiation

Fig. 1a

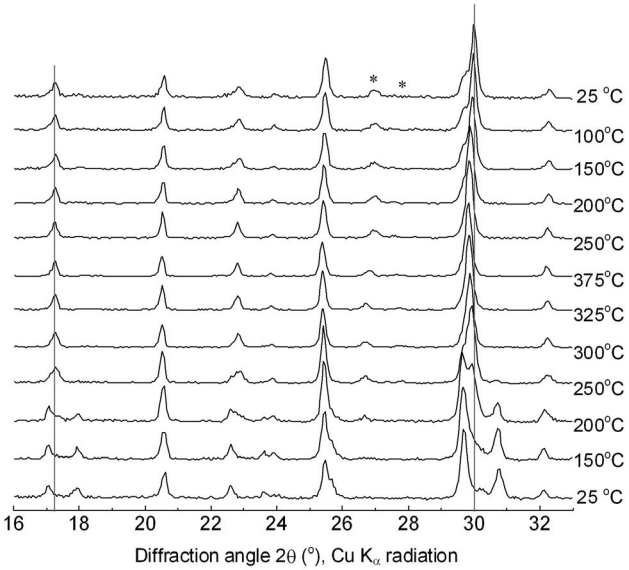
*
*
25 °C
100°C
150°C
200°C
250°C
375°C
325°C
300°C
250°C
200°C
150°C
25 °C
16
18
20
22
24
26
28
30
32
Diffraction angle 2θ (°), Cu Kα radiation

Fig. 1b

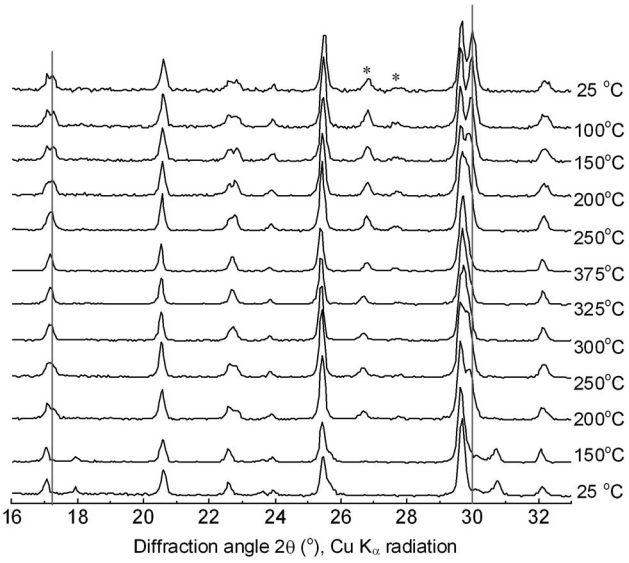
25 °C
100°C
150°C
200°C
250°C
375°C
325°C
300°C
250°C
200°C
150°C
25 °C
16 18 20 22 24 26 28 30 32
Diffraction angle 2θ (°), Cu Kα radiation

Fig. 1c

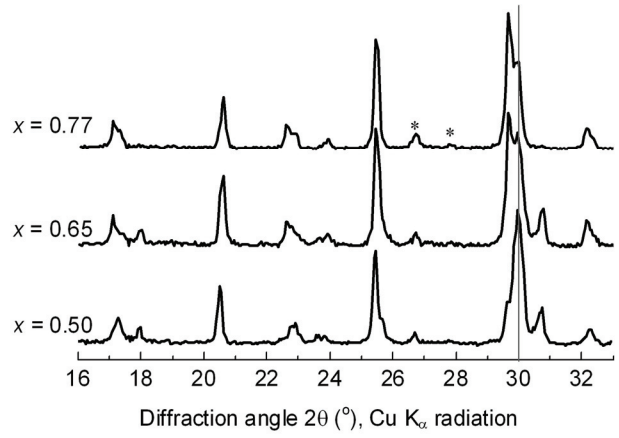
x = 0.77
x = 0.65
x = 0.50
16 18 20 22 24 26 28 30 32
Diffraction angle 2θ (°), Cu Kα radiation

Fig. 1d

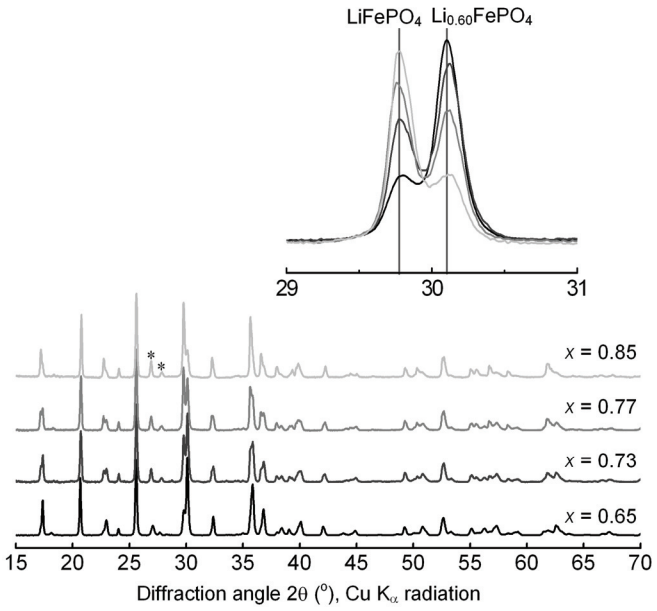
LiFePO4
Li0.60FePO4
29
30
31
x = 0.85
x = 0.77
x = 0.73
x = 0.65
15 20 25 30 35 40 45 50 55 60 65 70
Diffraction angle 2θ (°), Cu Kα radiation

Fig. 2a

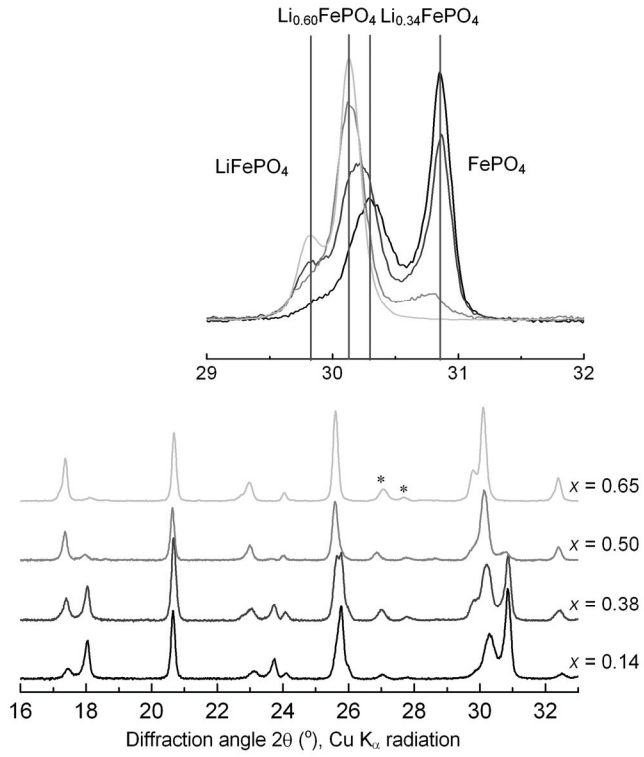
Li0.60FePO4
Li0.34FePO4
LiFePO4
FePO4
29
30
31
32
x = 0.65
x = 0.50
x = 0.38
x = 0.14
16 18 20 22 24 26 28 30 32
Diffraction angle 2θ (°), Cu Kα radiation

Fig. 2b

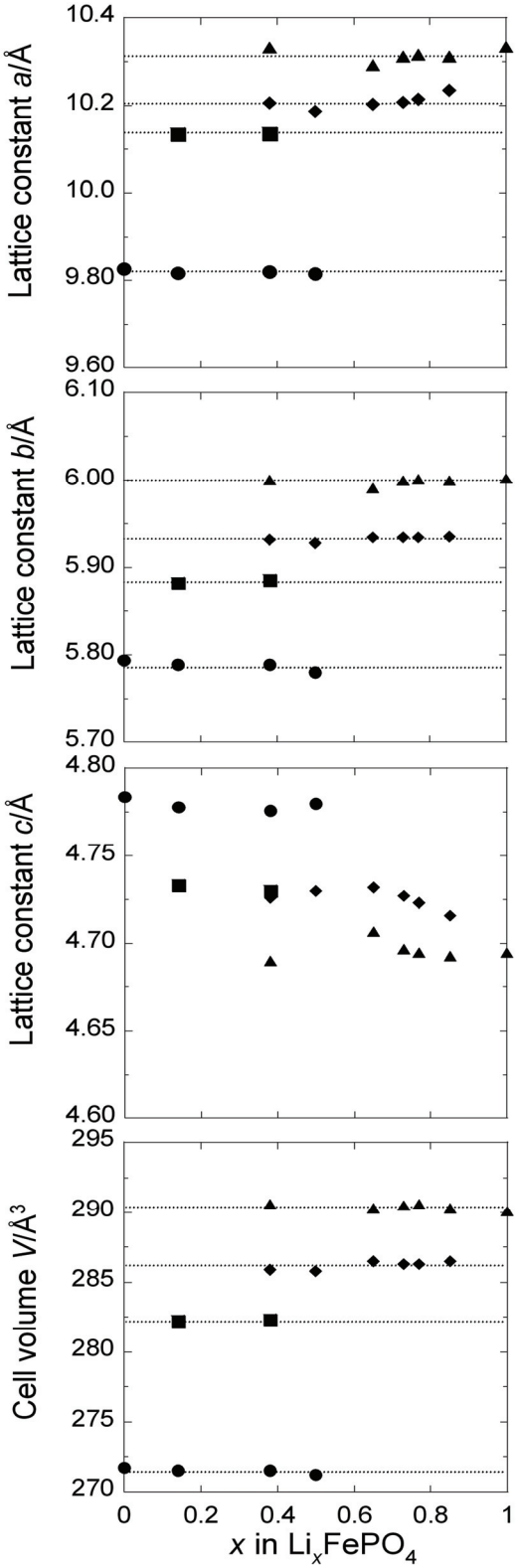
Lattice constant a/Å
10.4
10.2
10.0
9.80
9.60
Lattice constant b/Å
6.10
6.00
5.90
5.80
5.70
Lattice constant c/Å
4.80
4.75
4.70
4.65
4.60
Cell volume V/Å3
295
290
285
280
275
270
0
0.2
0.4
0.6
0.8
1
x in LixFePO4

Fig. 3

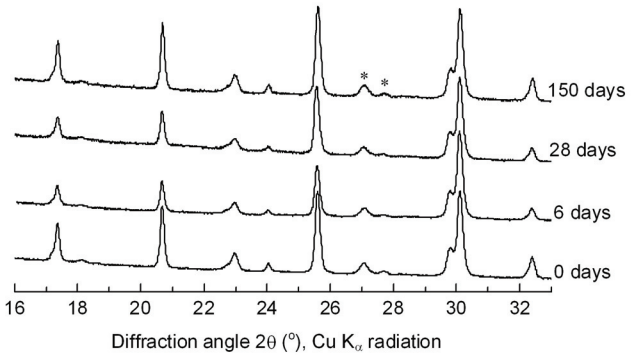
150 days
28 days
6 days
0 days
16
18
20
22
24
26
28
30
32
Diffraction angle 2θ (°), Cu Kα radiation

Fig. 4

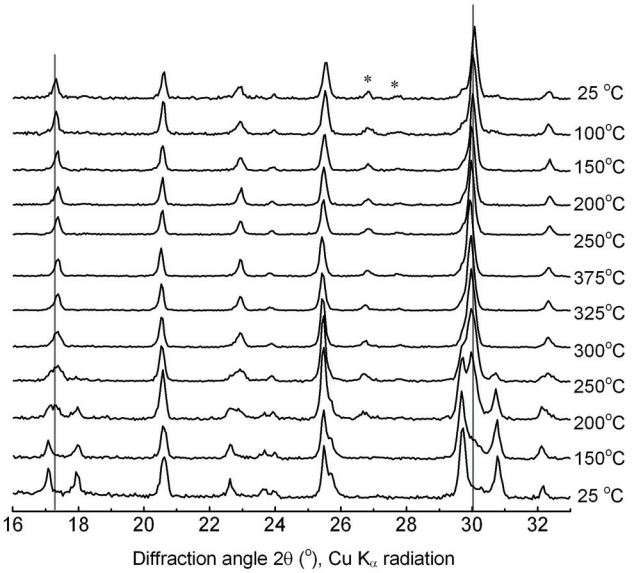
25 °C
100°C
150°C
200°C
250°C
375°C
325°C
300°C
250°C
200°C
150°C
25 °C
*
*
16
18
20
22
24
26
28
30
32
Diffraction angle 2θ (°), Cu Kα radiation

Fig. 5

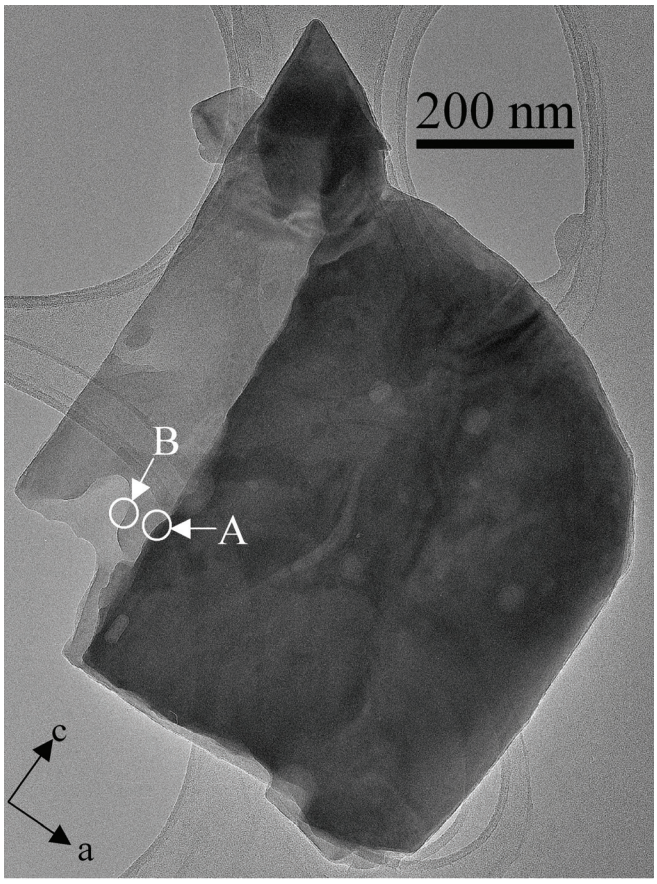

Fig. 6a

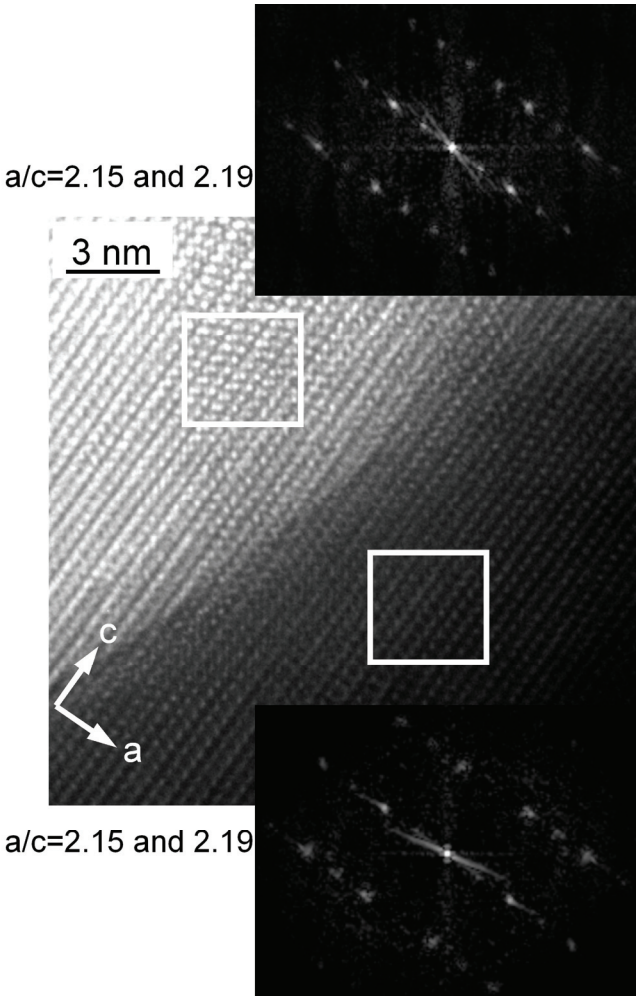

Fig. 6b